Journal of Integrative Agriculture 2026, 25(7): 2688–2700

Available online at ScienceDirect

Journal of Integrative Agriculture



RESEARCH ARTICLE

SBEIIb is responsible for the *chalk2* phenotype by regulating the formation of resistant starch in *indica* rice

Xinwei Li[1*], Zihang Wang[1*], Tianxiao Chen[1], Shen Lin[2], Guiai Jiao[1], Shaoqing Tang[1], Long Chen[1, 3], Xiangjin Wei[1#], Peisong Hu[1#]

[1] *State Key Laboratory of Rice Biology and Breeding/China National Center for Rice Improvement/China National Rice Research Institute, Hangzhou 311400, China*

[2] *Huaiyin Institute of Agricultural Science in Xuhuai Region of Jiangsu, Huai'an 223001, China*

[3] *Environment-friendly Crop Germplasm Innovation and Genetic Improvement Key Laboratory of Sichuan Province, Chengdu 610066, China*

Highlights

- A novel *OsSBEIIb* allele was identified in an *indica* rice mutant.
- The *OsSBEIIb* mutation increases the resistant starch (RS) content in raw rice flour, as well as in retrograded and heated rice.
- The *chalk2* mutant serves as a valuable *indica* rice germplasm for breeding high-RS rice varieties.

Abstract

Rice high in resistant starch is a valuable food for human health, especially for individuals with type 2 diabetes, as it supports effective blood sugar control and provides cardiovascular and intestinal benefits. However, developing rice varieties with a high resistant starch content remains a major challenge. In this study, we identified a mutant with increased chalkiness, *chalk2*, from the mutant library of *indica* rice Zhongjian 100. The *chalk2* mutants exhibited significantly higher amylose and protein contents, while the total starch and lipid contents were reduced. An analysis of resistant starch in *chalk2* revealed substantial increases in two resistant starch (RS) types, RS2 and RS3. Electron microscopy revealed abnormal starch granule development in the endosperm. The *chalk2* mutant also showed reduced grain length, width, and thickness, as well as a lower seed-setting rate, which ultimately led to a significant reduction in grain yield. Through physical localization, Mut-Map analysis, and transgene complementation, we found that *SBEIIb* was responsible for the *chalk2* phenotypes, and it is a member of the starch branching enzyme (SBE) family specifically expressed in the endosperm. Furthermore, the expression levels, enzymatic activity, and protein abundance of SBEIIb were significantly reduced in *chalk2* mutants. These findings suggest that *SBEIIb* plays a crucial role in regulating the composition of starch and resistant starch formation in *indica* rice.

Keywords: *Oryza sativa*, resistant starch, amylose, rice quality, rice yield

1. Introduction

Rice, one of the most important staple grains worldwide, has a high starch content (Amagliani *et al.* 2016). Starch serves as the primary energy reserve in grains and is the main source of carbohydrates in the human diet (Long *et al.* 2023). Rice starch is primarily composed of amylose and amylopectin (Miao and Hamaker 2021). Amylose is a linear compound made up of relatively long glucose chains, whereas amylopectin has a highly branched structure. Starch synthesis involves the complex interaction of several enzymes, including amylose synthesis catalyzed by granule-bound starch synthase (GBSS) and amylopectin formation mediated by starch synthase (SS), debranching enzymes (DB), and starch branching enzymes (SBE) (Ohdan *et al.*

Received 13 February 2025; Received in revised form 26 March 2025; Accepted 28 March 2025; Available online 18 April 2025
Xinwei Li, E-mail: lixinwei162013@163.com; [#]Correspondence Peisong Hu, Tel/Fax: +86-571-63370221, E-mail: peisonghu@126.com; Xiangjin Wei, Tel/Fax: +86-571-63370080, E-mail: weixiangjin@caas.cn
[*] These authors contributed equally to this study.

© 2026 CAAS. Publishing services by Elsevier B.V. on behalf of KeAi Communications Co. Ltd. This is an open access article under the CC BY-NC-ND license (http://creativecommons.org/licenses/by-nc-nd/4.0/). Peer review under responsibility of Editorial Board of *Journal of Integrative Agriculture*.
doi: 10.1016/j.jia.2025.04.026

2005; Tappiban *et al.* 2022; Wang L *et al.* 2023; Wang *et al.* 2025). With their distinct activity levels and genetic regulation in cereals, these enzymes play a key role in determining the structure and physicochemical properties of starch.

Researchers have identified a special class of starch known as resistant starch (RS) (Sajilata *et al.* 2006), which refers to starch that is not absorbed or digested in the normal human small intestine (Cummings and Englyst 1991). Based on its source and enzymatic properties, resistant starch is classified into five types: RS1 (physically encapsulated), RS2 (unripe starch), RS3 (retrograded starch), RS4 (chemically modified starch), and RS5 (lipid-complexed starch) (Turker and Savlak 2015). Resistant starch is considered a beneficial dietary fiber because it resists digestion in the small intestine and promotes gut motility, thereby improving intestinal health. When it reaches the large intestine, resistant starch is fermented by gut microbes into short-chain fatty acids (SCFAs). Butyrate, an SCFA produced during fermentation, has been shown to reduce the risk of colon cancer (Annison *et al.* 2003; Bird *et al.* 2004; Wang F *et al.* 2024). In individuals with diabetes, consuming resistant starch can significantly lower postprandial blood glucose levels and enhance insulin secretion. Long-term intake of foods high in resistant starch can improve insulin sensitivity and assist in weight management (Chisbert *et al.* 2024; Kim *et al.* 2024; Zhang 2024). Furthermore, resistant starch can reduce blood pressure, cholesterol, and triglycerides, making it a valuable component for cardiovascular disease prevention (Pugh *et al.* 2023; Wen *et al.* 2023). As a result, foods rich in resistant starch are gaining popularity as a healthy dietary choice.

Increasing the content of resistant starch in grains, especially rice, has become one of the key objectives for breeders. The SBE family plays a critical role in the formation of resistant starch in rice (Li *et al.* 2021; Utsumi *et al.* 2022; Biswas *et al.* 2023). Rice contains three main *SBE* genes: *SBEI*, *SBEIIa*, and *SBEIIb* (Yamanouchi and Nakamura 1992), which regulate different functions in controlling the degree of starch polymerization. *SBEI* mainly transfers short chains with a degree of polymerization (DP) between 11 and 22, while *SBEIIa* is involved in transferring short to medium chains (DP 6–15), and *SBEIIb* transfers short chains with DP values between 6 and 7 (Nakamura *et al.* 2010). Notably, while *SBEIIa* can partially compensate for the function of *SBEI*, it cannot compensate for the function of *SBEIIb* (Sawada *et al.* 2018). SBEIIb has been widely recognized for its role in controlling resistant starch formation in *japonica* rice. The loss of SBEIIb activity leads to a significant increase in resistant starch in the rice endosperm. For instance, the loss of *OsSBEIIb* function in the *japonica* rice mutant *em10* resulted in a dramatic increase in the resistant starch and amylose contents (Nishi *et al.* 2001). This mutant has been used to create the new rice variety Chikushi-kona 85, which has a resistant starch content of up to 17.4% (Wada *et al.* 2018). In *japonica* rice, CRISPR-Cas9 technology has been employed to knock down *OsSBEIIb* expression, leading to higher resistant starch and amylose contents in the rice endosperm (Sun *et al.* 2017; Guo *et al.* 2020). In addition, researchers have used RNAi to reduce the expression of *OsSBEIIb* in the *japonica* rice variety Nipponbare, resulting in a 4.8% increase in resistant starch and a 42.0% increase in amylose content in the endosperm (Butardo *et al.* 2011). The role of *OsSBEIIb* in increasing amylose content and influencing RS synthesis by altering the starch chain length distribution has been reported in *japonica* rice. However, studies involving the forward genetic cloning of *OsSBEIIb* alleles in *indica* rice remain limited. While a previous study achieved higher RS content by knocking out *OsSBEIIb* in the *rs4* mutant (a γ-ray-induced mutant of *indica* rice R7954 with pre-existing *SSIIIa* and *SSIIIb* mutations) (Wang A *et al.* 2023; Wang A Q *et al.* 2024), this study identifies a novel *OsSBEIIb* mutant directly from an ethylmethanesulfonate (EMS)-induced *indica* rice mutant library, offering novel genetic resources for breeding high-RS *indica* rice.

In this study, we cloned the *OsSBEIIb* gene involved in endosperm starch biosynthesis from the *indica* rice cultivar Zhongjian 100 (ZJ100). We uncovered the pivotal role of *OsSBEIIb* in regulating starch composition and resistant starch formation in rice endosperm. Ultimately, we identified a valuable *indica* rice germplasm with high resistant starch content that holds significant potential for developing high resistant starch rice varieties.

2. Materials and methods

2.1. Plant materials and growth conditions

The *chalk2* mutant was identified from an EMS-treated population of *indica* rice cultivar ZJ100. Two F_2 populations were generated from crosses between *chalk2*×*japonica* rice cultivar Zhonghua 11 (ZH11) and *chalk2*×ZJ100 and used for gene mapping. All plants, including the transgenic lines, were grown under natural conditions in paddy fields in Hangzhou, Zhejiang Province, China.

2.2. Measurement of grain-filling rate

At noon on the day of peak flowering in rice, the flowering glumes were marked with a black pen. Samples are taken on the 5th, 10th, 15th, 20th, and 25th days after fertilization (DAF). The seeds were then directly dried in an oven at 65°C until they reached a constant weight, and then they were hulled, and weighed. Each sample was repeated three times to measure the dry matter accumulation during endosperm filling.

2.3. Microscopic observation

To observe the development and structure of compound starch grains, transverse sections of ZJ100 and *chalk2* at 6 and 9 DAF were used to prepare semi-thin sections (no thicker than 1 mm). The samples were stained with a 1% I-KI solution for 5 s and then examined under a microscope. Brown rice grains were transversely cut in the middle using a knife to prepare the samples. Images were captured using an S3400N scanning electron microscope (Hitachi, Tokyo, Japan).

2.4. Physicochemical property analysis of rice

The total starch and amylose contents were measured using a Starch Assay Kit (Megazyme, Wicklow, Ireland). Lipid and total protein contents in the grains were determined following

the method described by Kang *et al.* (2005). To assess the starch pasting properties, 3 g of milled rice powder was mixed with 25 mL of distilled water in a container. The sample was then analyzed using a rapid visco analyzer (Newport Scientific, Narrabeen, NSW, Australia). For gelatinization temperature analysis, 5 mg of milled rice flour was weighed, sifted through a 100-mesh sieve, and placed in an aluminum sample pan, while ensuring that the sample was concentrated at the bottom and not adhering to the pan walls. Then, 10 μL of double-distilled water was added to ensure even hydration of the sample. The pan was sealed with an aluminum lid to prevent moisture evaporation. The measurement was taken using a differential scanning calorimeter (DSC1; Mettler Toledo, Greifensee, Switzerland) with a heating rate of 10°C min^{-1} and a temperature range of 35–100°C. A sealed empty aluminum pan was used as a reference. The swelling behavior of endosperm starch in urea solution was measured according to previously reported methods (Wei *et al.* 2017).

2.5. Mapping and cloning of the gene responsible for the *chalk2* mutant

A total of 138 polymorphic simple sequence repeat (SSR) markers between *chalk2* and ZH11 were used for linkage mapping in the F_2 population of *chalk2*×ZH11 (Appendix A). Among them, six polymorphic SSR markers were specifically associated with the *chalk2* phenotype. The MutMap method, as described by Abe *et al.* (2012), was then applied to fine map the locus. A pool of 30 individuals with the mutant phenotype was selected from the F_2 population derived from *chalk2*×ZJ100, with ZJ100 serving as the dominant pool. Both DNA samples underwent whole-genome sequencing using the Illumina Xplux platform (LC-BIO, Hangzhou, China). Short reads were aligned to the Nipponbare reference genome (MSU 7.0) to identify reliable SNPs. SNP index plots were generated by averaging the scores in a sliding 2 Mb window with 10 kb increments. Candidate SNPs with an SNP index greater than 0.8 were selected for further screening. SSR and insertion/deletion markers with polymorphisms between ZJ100 and ZH11 were used to identify markers linked to the candidate gene (Table 1).

2.6. Vector construction and plant transformation

The full-length DNA sequence of *OsSBEIIb* and its 1.5 kb natural promoter from ZJ100 was isolated by PCR and subsequently subcloned into the binary vector pCAMBIA1300. The resulting plasmids were introduced into *Agrobacterium tumefaciens* strain EHA105, which was then used to transform the *chalk2* mutant *via Agrobacterium*-mediated transformation. The genotypes of the transgenic plants were confirmed by PCR amplification of the *neomycin phosphotransferase II* (*NPTII*) gene. The primers used for vector construction are listed in Table 1.

2.7. RNA extraction and real-time PCR (RT-PCR) expression analysis

Total RNA was extracted from roots, shoots, stems, leaves, spikes, and developing seeds at 5, 10, 15, 20, and 25 DAF using the RNAprep Pure Plant Kit (TIANGEN Biotech, Beijing, China). A total of 2 μg of total RNA was reverse transcribed using oligo (dT) primers in a 40 μL reaction, following the instructions of the PrimeScript Reverse Transcriptase Kit (TaKaRa, Japan; http://www.takara-bio.com). Gene expression was quantified using quantitative real-time PCR (qRT-PCR), with the *Ubiquitin* gene (GenBank accession AF184280) as an internal reference. PCR amplification was performed on an ABI 7500 Fast Real-Time PCR System using the following program: 95°C for 30 s, followed by 40 cycles of 95°C for 5 s, 60°C for 34 s, and 95°C for 15 s. Changes in gene expression were calculated using the $2^{-\Delta\Delta CT}$ method (Wei *et al.* 2017). The primers used for qPCR are listed in Table 1.

2.8. Subcellular localization

The cDNA of *Chalk2*, excluding the terminator, was cloned into the pYBA1132-GFP vector, with positioning of the *Chalk2* gene upstream of the *GFP* coding sequence, to construct a Chalk2-GFP fusion protein under the control of the cauliflower mosaic virus (CaMV) 35S promoter. The fusion construct and an empty control vector (pYBA1132-GFP) were each transformed into rice protoplasts. GFP fluorescence signals were observed using a confocal laser scanning microscope (Leica TCS SP5, Germany; http://www.leica.com). The primers used for vector construction are listed in Table 1.

2.9. SBE and GBSS enzymatic activity assays

For enzymatic activity measurement, 100 mg of developing seeds from both wild-type (WT) and mutant plants were harvested at 10 DAF. The seeds were then homogenized

Table 1 Primers used in this study

Name	Forward (5′→3′)	Reverse (5′→3′)
Primers for map-based cloning		
RM6233	AGAACGGCGACACGTGGAC	ACGATGACGCCCATGATG
RM12923	AAATGCACAGGCATTCGTAGACC	GAAGAAGTGGATGGAGGACATGG
RM13069	GGAGGGTTATTCTCGCGTAAAGG	GACCCTTCACATTTCGGTCAGC
RM221	ACATGTCAGCATGCCACATC	TGCAAGAATCTGACCCGG
RM573	CCAGCCTTTGCTCCAAGTAC	TCTTCTTCCCTGGACCACAC
RM318	GTACGGAAAACATGGTAGGAAG	TCGAGGGAAGGATCTGGTC
Primers for *Chalk2* expression patterns		
RT-*Chalk2*	TGCTGAGCAGAAACCACGAG	ATGTCTGAACGCAGTCTCCT
Primers for vector construction		
1132-*Chalk2*	CGGGCTGCAGGAATTCATGGCGGCGCCGGCGTCTGC	TGCTCACCATGGTACCTTCCGCTGGAGCATAGACAA
1300-*Chalk2*	CCGGGGATCCTCTAGACATGTCACCAGCTCCACGAT	TGCCTGCAGGTCGACGCGGCAGTGCGTATTAACAAG

on ice in 1 mL of extraction buffer using a mortar. Enzymatic activity was measured using specific assay kits (SBE-2-Y, GBSS-2B-Y, Cominbio) according to the manufacturer's instructions. Finally, the activities of the GBSS and SBE enzymes were determined by measuring absorbance at wavelengths of 340 and 660 nm, respectively.

2.10. Plant protein extraction and Western blot analysis

To extract total protein, grains were collected at 10 DAF and homogenized in 1.5 mL of extraction buffer. The supernatant containing total protein was obtained by centrifugation. Equal amounts of protein were then separated on an SDS-PAGE gel, transferred onto a polyvinylidene (PVDF) membrane, and immunoblotted using the appropriate antibodies. The specific bands were detected using an enhanced chemiluminescence detection kit (Thermo Fisher Scientific, USA). These protein fractions were loaded onto an SDS-PAGE gel for immunoblot analysis, with SBEIIb, GBSSI, and *β*-actin serving as internal controls.

2.11. Analysis of resistant starch in grains

Mature seeds were harvested and air-dried until the moisture content reached 12%. The dried seeds were then ground into rice flour. The resistant starch type 2 (RS2) content was measured directly from the rice flour. For the preparation of RS3, 0.1 g of complete milled rice was weighed, and 2 mL of distilled water was added. The mixture was boiled for 20 min, kept warm for 20 min, and then allowed to cool at room temperature for 24 h. The resistant starch content in hot-cooked rice was measured directly, excluding the cooling process. The determination of resistant starch followed a previously established protocol, using the resistant starch assay kit according to the manufacturer's instructions (Megazyme, Wicklow, Ireland).

3. Results

3.1. Chalkiness and yield performance of *chalk2*

The *chalk2* mutant showed a significant increase in the number of opaque seeds in brown rice, with a distinctive white center (Fig. 1-A). Statistical analysis of the mutant's chalkiness rate and degree revealed marked increases in both parameters compared to ZJ100 (Fig. 1-E and F). The *chalk2* mutant exhibited a slower grain-filling rate and lower grain dry weight between 10 to 25 DAF compared to ZJ100 (Fig. 1-C and D). Regarding grain morphology, the *chalk2* mutant had significantly smaller grain length, width, and thickness compared to ZJ100 (Fig. 1-G), resulting in a significant reduction in thousand-grain weight (Fig. 1-H). Throughout the entire growth and development period, no significant changes were observed except for a notable reduction in plant height in the *chalk2* mutant, and the *chalk2* mutant was significantly shorter than ZJ100 (Fig. 1-B and I). There were no significant differences in tiller number or number of grains per panicle between *chalk2* and ZJ100 (Fig. 1-J and K), but the seed-setting rate of *chalk2* was approximately 10% lower than that of ZJ100 (Fig. 1-L). Consequently, due to these changes in seed-setting rate and thousand-grain weight, the yield per plant in the *chalk2* mutant was significantly lower than that in ZJ100 (Fig. 1-M).

3.2. Endosperm starch accumulation and physico-chemical properties in *chalk2*

Scanning electron microscope (SEM) analysis revealed that the starch grains (SGs) in mature endosperm cells of the *chalk2* mutant contained loosely arranged, spherical SGs (Fig. 2-A). In ZJ100, the SGs were irregular, polyhedral, and square-shaped (Fig. 2-B). In addition, the developing endosperm was examined at 6 and 9 DAF using semi-thin sections. At 6 DAF, the space between SGs in the *chalk2* mutant was found to be significantly larger than in ZJ100 (Fig. 2-C and D). A similar pattern was observed at 9 DAF, where the SGs in the ZJ100 endosperm were densely arranged, while the *chalk2* mutant exhibited loosely packed SGs, with significantly larger spaces between individual endosperm cells compared to ZJ100 (Fig. 2-D–F).

The transformation of the endosperm starch morphological structure in the mutant influenced rice quality. The total starch and lipid contents in the endosperm of *chalk2* were significantly lower than in ZJ100 (Fig. 2-G and J). In contrast, the amylose and protein contents were significantly higher in the *chalk2* mutant, with amylose content increasing by nearly 10% (Fig. 2-H and I). The physicochemical properties of starch in the endosperm of both ZJ100 and the *chalk2* mutant were also analyzed. The gelatinization consistency of ZJ100 was notably longer than that of the *chalk2* mutant (Fig. 2-K). The starch solubility in urea was assessed by mixing starch powder with different concentrations (0–9 mol L^{-1}) of urea solution. The results showed that the *chalk2* mutant was difficult to gelatinize even in 6 mol L^{-1} urea, whereas ZJ100 starch easily gelatinized at concentrations between 5 and 9 mol L^{-1} (Fig. 2-M). The viscosity profiles of ZJ100 and *chalk2* differed significantly. Before the temperature reached 100°C, ZJ100 exhibited higher viscosity that peaked at 100°C, whereas the *chalk2* mutant showed a lower initial viscosity. However, as the temperature decreased and time increased, the viscosity of ZJ100 dropped below that of *chalk2*, which continued to rise (Fig. 2-L). The gelatinization temperatures of starch in ZJ100 and the *chalk2* mutant were measured using differential scanning calorimetry (DSC). The results indicated that the onset temperature (T_o), peak temperature (T_p), end temperature (T_e), and gelatinization enthalpy (ΔH) of the *chalk2* endosperm starch were significantly higher than those of ZJ100. Analysis of the chain length distributions of amylopectin in ZJ100 and *chalk2* revealed a reduction in short-chain amylopectin (6<DP<12) and an increase in medium- to long-chain amylopectin (13<DP<30) (Fig. 2-O). These findings suggest that the starch composition and physicochemical properties of *chalk2* differ markedly from those of ZJ100.

3.3. Gene responsible for the *chalk2* mutation

A linkage mapping and Mut-Map combination method was used to identify the gene responsible for the *chalk2* mutation phenotype (Fig. 3-A). First, the *chalk2* locus was localized to between the markers RM13069 and RM221 on the long arm of chromosome 2 by linkage mapping. Next, 30 individuals with a high chalkiness rate were selected from the F_2

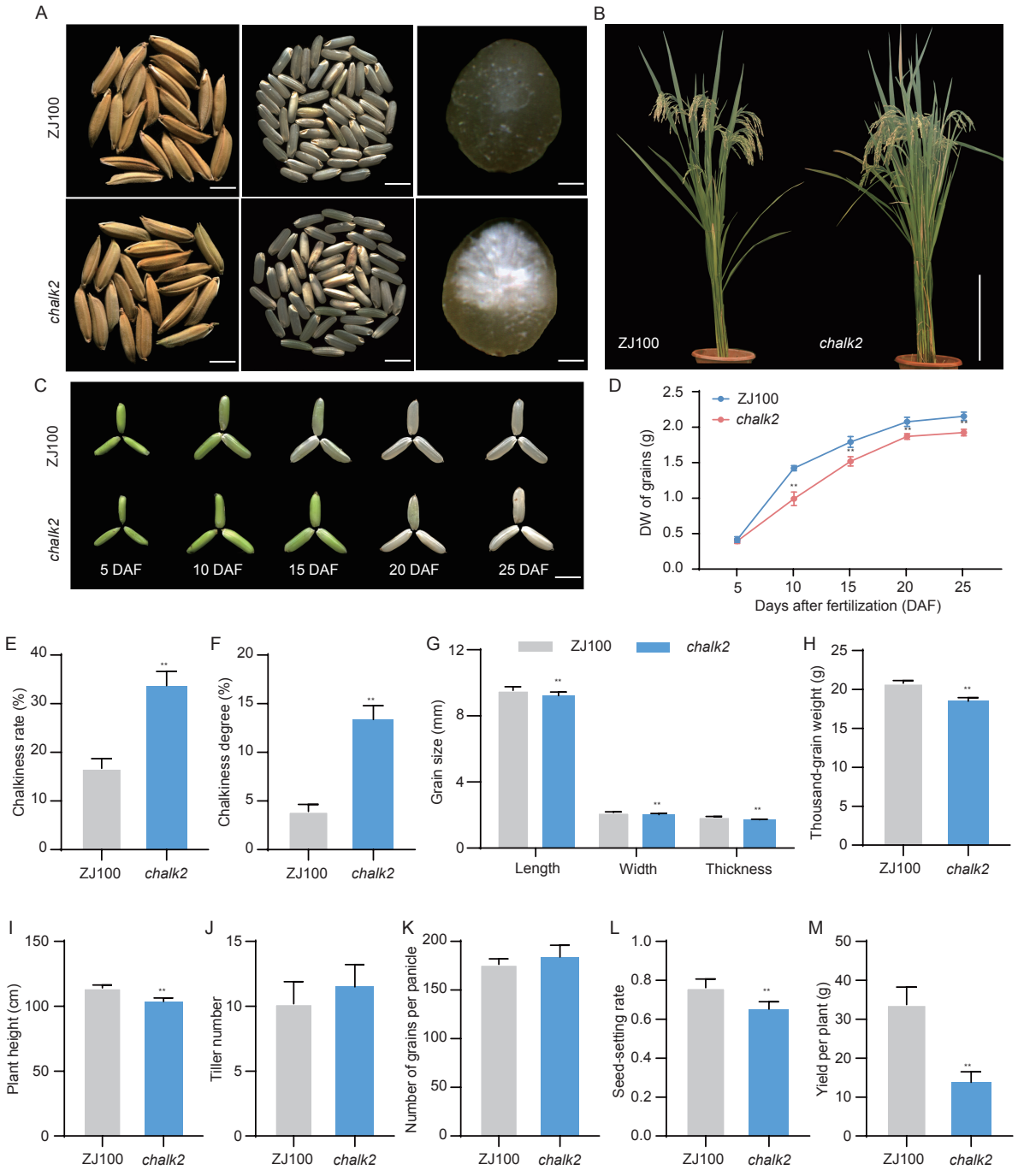


Fig. 1 Characterization of the *chalk2* mutant. A, left, grain appearance of Zhongjian 100 (ZJ100) and the *chalk2* mutant. Scale bars, 0.5 cm. Middle, brown rice appearance of ZJ100 and the *chalk2* mutant. Scale bars, 1 cm. Right, brown rice cross-section appearance of ZJ100 and the *chalk2* mutant. Scale bars, 5 mm. B, plant phenotypes of ZJ100 and the *chalk2* mutant. Scale bars, 30 cm. C, fresh grains of ZJ100 and *chalk2* at various stages of development. DAF, days after fertilization. Scale bars, 1 cm. D, dry weight (DW) of grains of ZJ100 and *chalk2* at various stages. E and F, chalkiness rate (E) and chalkiness degree (F) of ZJ100 and *chalk2*. G–M, grain size (G), thousand-grain weight (H), plant height (I), tiller number (J), number of grains per panicle (K), seed-setting rate (L), and yield per plant (M) of ZJ100 and *chalk2*. Data in D–F are shown as mean±SD from at least three replicates, and in G–M data are shown as mean±SD from at least 10 replicates. ** indicates significant difference at $P<0.01$ by the two-tailed Student's *t*-test.

population of *chalk2*×ZJ100. The DNA of these individuals displaying the mutant phenotype were bulked and subjected to whole-genome sequencing, along with WT plants (ZJ100). In the primary mapping region on chromosome 2, a single peak was identified that contained five SNPs with an index greater than 0.8 (Fig. 3-A). Among these SNPs, a nonsynonymous SNP (G to A) in the 16th exon of *LOC_Os02g32660* in the *chalk2* mutant caused a substitution of serine to asparagine (Fig. 3-B). According to the Rice Genome Annotation Project (https://rice.uga.edu/index.shtml), *Chalk2* (*LOC_Os02g32660*) encodes the 1,4-alpha-glucan-branching enzyme *OsSBEIIb*.

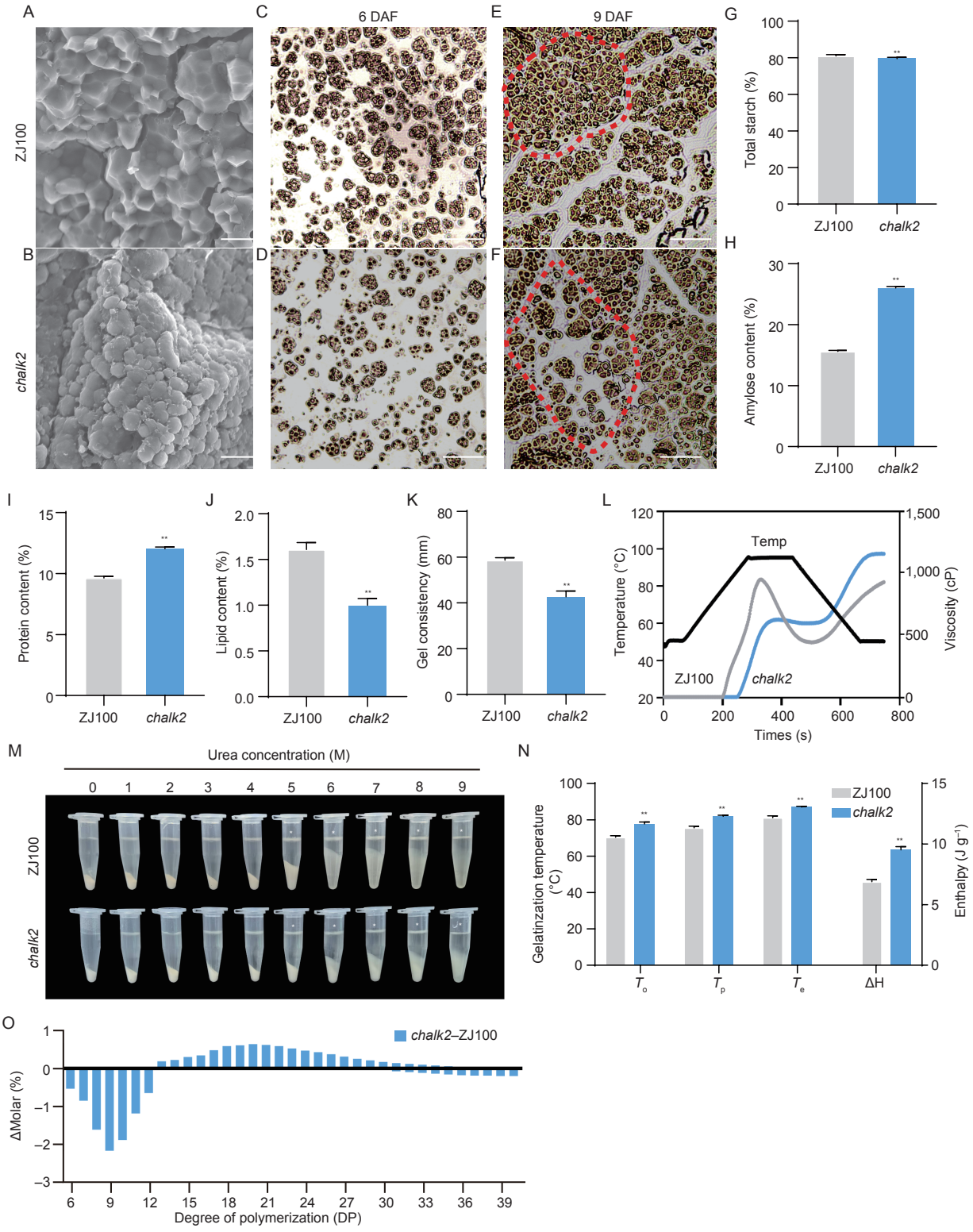


Fig. 2 Starch granule accumulation and characteristics of *chalk2* grains and physicochemical properties of starch in Zhongjian 100 (ZJ100) and the *chalk2* mutant. A and B, scanning electron microscope (SEM) images of transverse sections of ZJ100 (A) and *chalk2* (B) endosperm cells. Scale bars, 30 μm. C–F, semi-thin sections of ZJ100 (C and E) and *chalk2* (D and F) endosperm cells. DAF, days after fertilization. Scale bars, 100 μm. G–L, the contents of total starch (G), amylose (H), protein (I), lipid (J), gel consistency (K), and viscosity (L) in ZJ100 and *chalk2*. Blue and gray lines, pasting properties of endosperm starch in the *chalk2* mutant (blue line) and ZJ100 (gray line). The viscosity value at each temperature is the average of three replicates. The black line indicates the temperature fluctuation during the measurements. M, starch of *chalk2* grains is difficult to gelatinize in urea solution. Starch powder was mixed with different concentrations (0 to 9 mol L^{-1}) of urea solution. Each asterisk indicates a distinct centrifugal tube. N, thermal gelatinization temperature of endosperm starch in ZJ100 and *chalk2*. T_o, T_p, T_e, and ΔH represent the onset, peak, and conclusion gelatinization temperatures and gelatinization enthalpy, respectively. Data in G–L and N are shown as mean±SD from at least three replicates. ** indicates significant differences at $P<0.01$ by the two-tailed Student's *t*-test. O, differences in the distribution of amylopectin chain lengths between ZJ100 and the *chalk2* mutant.

To confirm whether *LOC_Os02g32660* (*Chalk2*, *OsSBEIIb*) was the candidate gene responsible for the mutant phenotype, the *chalk2* mutant was transformed with a complementation vector carrying the *OsSBEIIb* genomic sequence, including its native promoter. For further verification, relative expression analysis was performed *via* qRT-PCR using total plant RNA from ZJ100, *chalk2*, and two of the complementation transgenic lines (COM1 and COM2). The results showed that the relative expression in *chalk2* was significantly lower than in ZJ100, while the COM1 and COM2 lines exhibited expression levels nearly identical to ZJ100 (Fig. 3-D). In addition, the phenotypes of the COM1 and COM2 lines, including chalkiness rate, chalkiness degree, and thousand-grain weight, were similar to ZJ100 (Fig. 3-C,

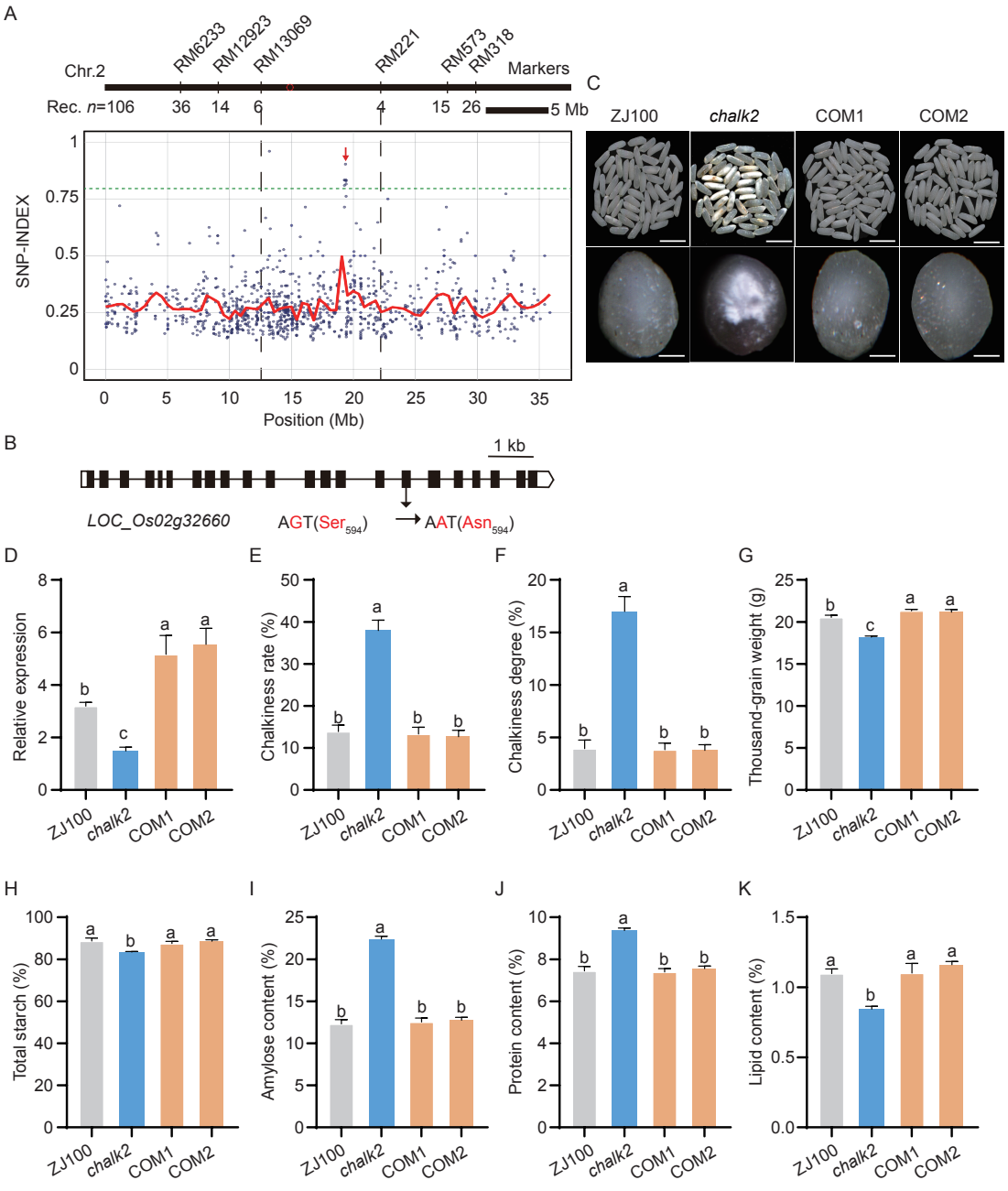


Fig. 3 Identification of *chalk2* by linkage mapping and the Mut-Map method. A, the *Chalk2* locus was first mapped to the long arm of chromosome 2 between the markers RM13069 and RM221. Genomic regions possibly harboring causal mutations for *chalk2* mutants were identified using Mut-Map. The red curves represent SNP index plots on chromosome 2; and the red arrow indicates a single peak detected in the primary mapping region. B, gene structure and mutation site in *Chalk2* (*LOC_Os02g32660*). A SNP (G to A) causes a change of Ser-594 to Asn-594 in the encoded protein. C, milled rice and cross-sectional appearance of Zhongjian 100 (ZJ100), the *chalk2* mutant and the complementation lines (COM1 and COM2). Scale bars, 1 cm (above), 5 mm (below). D, relative expression levels of *Chalk2* in the developing endosperms of ZJ100, *chalk2*, and the COMs. E–K, data for the chalkiness rate (E), chalkiness degree (F), thousand-grain weight (G), total starch content (H), amylose content (I), protein content (J), and lipid content (K) of ZJ100, *chalk2* and the COMs. Data in E–K are shown as mean±SD from at least three replicates. Different letters indicate significant differences at $P<0.01$ by one-way ANOVA with Bonferroni correction.

E, and G). Finally, rice quality was analyzed in the COM1 and COM2 lines. The results showed that the contents of total starch, amylose, lipid, and protein in the COM lines were similar to those in ZJ100 (Fig. 3-H–K). All these results indicate that *OsSBEIIb* is responsible for the alterations observed in the *chalk2* mutant.

3.4. Spatio-temporal expression pattern and subcellular localization in *Chalk2*

The SMART website (https://smart.embl.de/) was used to analyze the domains of the Chalk2 protein (OsSBEIIb). The results showed that *Chalk2* encodes a protein of 825 amino acids that contains three Pfam domains: CBM_48 (from 191–275 aa), Alpha-amylase (from 337–441 aa), and Alpha-amylase_C (from 729–824 aa) (Fig. 4-A). Two other SBE homologous proteins are known in *Oryza sativa japonica*: OsSBEI and OsSBEIIa. The phylogenetic tree indicated that OsSBEIIb has been conserved in the evolutionary process of these species (Fig. 4-B). In addition, a multiple sequence alignment of OsSBEIIb homologous proteins revealed that the *chalk2* mutation is located in a highly conserved region (Fig. 4-C). Although the mutation site is not located within the CBM_48, Alpha-amylase, or Alpha-amylase_C domains, it still affects the protein structure (Appendix B).

Next, the 35S::Chalk2-GFP fusion expression protein was constructed to determine the subcellular localization of Chalk2. The results showed that the GFP signal from Chalk2-GFP was localized in the chloroplasts (Fig. 4-D). To obtain more precise results, a 35S::GBSSI-CFP fusion protein was constructed, as GBSSI is a plastid-localized protein, and it was co-transformed with Chalk2-GFP into rice protoplasts. The results showed that GFP fluorescence, CFP fluorescence, and chloroplast autofluorescence overlapped (Fig. 4-E). Furthermore, total RNA from ZJ100 was extracted and qRT-PCR analysis was performed on samples from roots, shoots, stems, leaves, spikes, and seeds (from 6

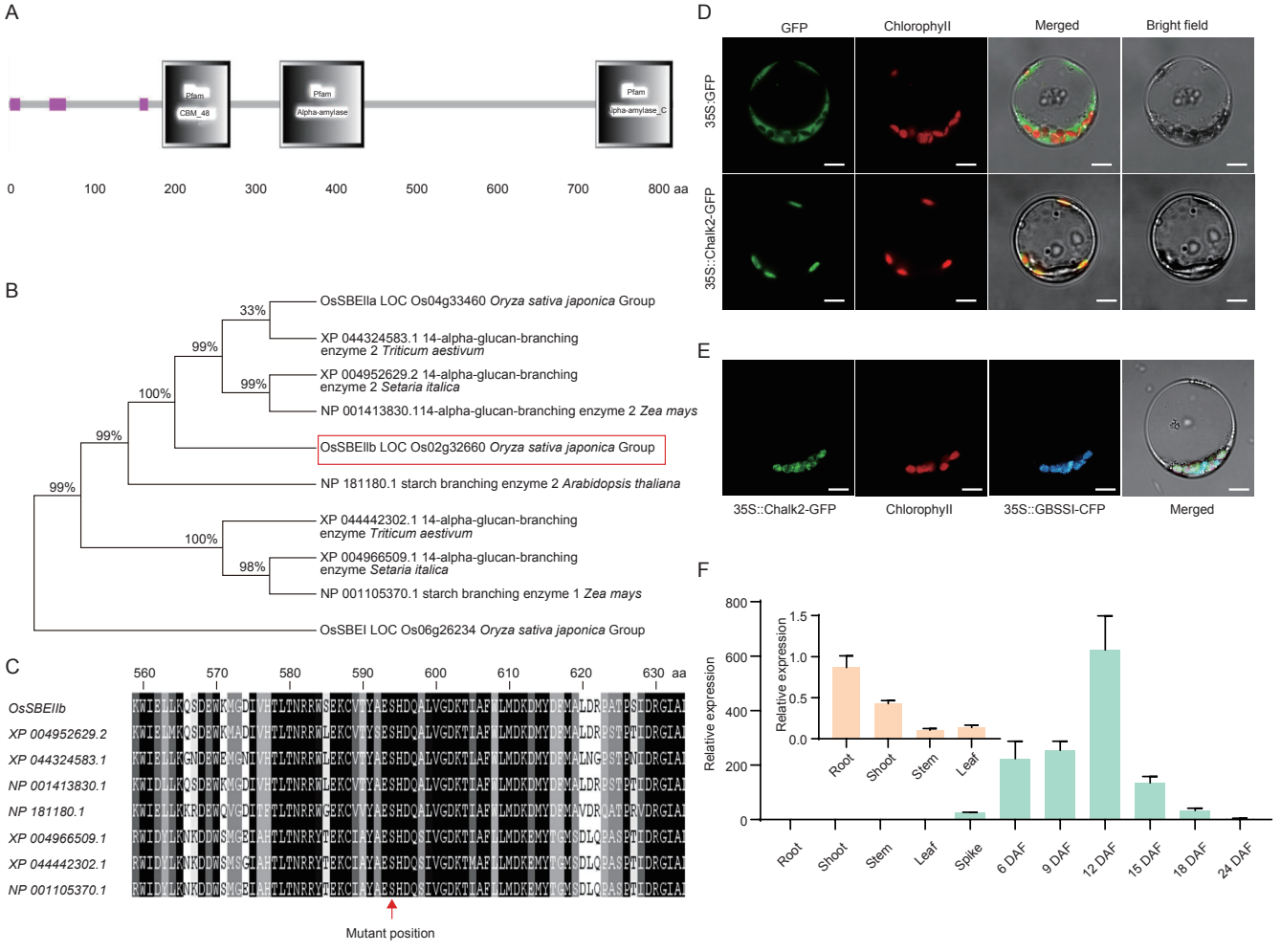


Fig. 4 *Chalk2* bioinformatics analysis, subcellular localization and expression patterns. A, schematic domain structure of the Chalk2 protein. B, phylogenetic analysis of the starch branching enzymes (SBE) family. C, multiple sequence alignment of OsSBEIIb homologous proteins. D, subcellular localization of the Chalk2 protein. Rice protoplast cell expressing GFP alone (upper panels); protoplast cell expressing 35S::Chalk2-GFP (lower panels). From left to right: GFP signal of the fusion protein, chloroplast autofluorescence, chloroplast autofluorescence, the merged image of the GFP signal, and its bright field image. Scale bars, 5 μm. E, colocalization of Chalk2-GFP and GBSSI-CFP. From left to right, GFP signal, chloroplast signal, CFP signal, and the merged signal. Scale bars, 5 μm. F, tissue-specific expression patterns revealed by real-time PCR. RNA was isolated from various tissues of ZJ100. The *Ubiquitin* gene (GenBank accession AF184280) served as the internal control. DAF, days after fertilization. Data in F are shown as mean±SD from at least three replicates.

to 24 DAF). The results indicated that *Chalk2* is highly expressed in seeds, particularly at 12 DAF, with almost no expression detected in the stems or leaves (Fig. 4-F). These findings suggest that Chalk2 (OsSBEIIb) is a plastid-localized protein that is highly expressed in seeds and conserved across species.

3.5. SBE enzymatic activity and protein abundance in *chalk2*

The starch branching enzymatic activity was examined using 12 DAF grains from ZJ100, *chalk2*, and COM1. The results showed that SBE enzymatic activity in *chalk2* was significantly lower than in ZJ100 and COM1, while no significant difference was observed between ZJ100 and COM1 (Fig. 5-A). GBSSI is the primary enzyme responsible for amylose synthesis. As the amylose content was significantly higher in *chalk2*, the GBSSI enzymatic activity was also analyzed in 12 DAF grains from ZJ100, *chalk2*, and COM1. The results revealed that GBSSI enzymatic activity was significantly higher in *chalk2* compared to ZJ100 and COM1 (Fig. 5-B).

In addition, total protein extracted from 12 DAF grains was subjected to western blot analysis. The results showed that the protein abundance of SBEIIb decreased, while the protein abundance of GBSSI increased in *chalk2*, aligning with the observed enzymatic activity changes in *chalk2* (Fig. 5-C). These results suggest that *Chalk2* influences starch synthesis by modulating enzymatic activities.

3.6. Content of resistant starch in the *chalk2* mutant

An increase in the amylose content of rice grains is closely linked to changes in resistant starch content (Sun *et al.* 2017; Guo *et al.* 2020). Resistant starch can be classified into five types, with RS2 and RS3 being the most common. In this study, the RS2 contents in brown and milled rice (Fig. 6-A and B), and the RS3 content in retrograded rice were measured (Fig. 6-C). In addition, the contents of resistant starch in hot-cooked rice were examined in the *chalk2* mutant, ZJ100, and COM1 (Fig. 6-D). The results showed that the RS2 contents in both brown and milled rice increased more than 40-fold in the *chalk2* mutant compared to ZJ100 and COM1. A similar trend was observed for RS3 in retrograded rice from the mutant, ZJ100, and COM1. In hot-cooked rice, the increase in RS was also significant in the mutant. Overall, these findings suggest that *Chalk2* is involved in the synthesis of resistant starch and our *chalk2* mutant can be used as a valuable germplasm resource to increase the RS content of rice varieties.

3.7. Expression of key starch synthesis genes in the *chalk2* mutant

qRT-PCR was performed to analyze the expression levels of a series of genes involved in starch biosynthesis and metabolism. The results showed that in the *chalk2* mutant, the expression levels of genes associated with starch precursor synthesis (*AGPL1*, *AGPL2*, and *AGPS1*) were significantly upregulated, suggesting that the *chalk2* mutation may enhance the accumulation of starch precursor metabolites. Furthermore, the expression level of *FLO6*, a gene containing the CBM48 domain, was markedly downregulated, implying that this mutation may affect starch granule formation in the endosperm.

Among the isoamylase (*ISA*) gene family members, changes in the expression levels of *ISA1* and *ISA2* suggested that the *chalk2* mutation might disrupt the dynamic balance of debranching enzymes. In the *SBE* gene family, the expression levels of *SBEI* and *SBEIIa* were significantly downregulated. Similarly, the expression levels of genes related to starch degradation, including members of the α-amylase gene family (*Amy3A*, *Amy3B*, and *Amy3E*), were also markedly reduced. In the *SS* gene family, the expression levels of *SSIIIa* and *SSIIIb* were significantly upregulated, with *SSIIIa* showing the highest fold increase. These alterations in the expression of key genes involved in starch biosynthesis and metabolism may provide further insights into the substantial increase in RS content observed in the *chalk2* mutant.

4. Discussion

4.1. *OsSBEIIb* regulates starch synthesis and physico-chemical properties

Starch is the main storage substance in rice grains, and the

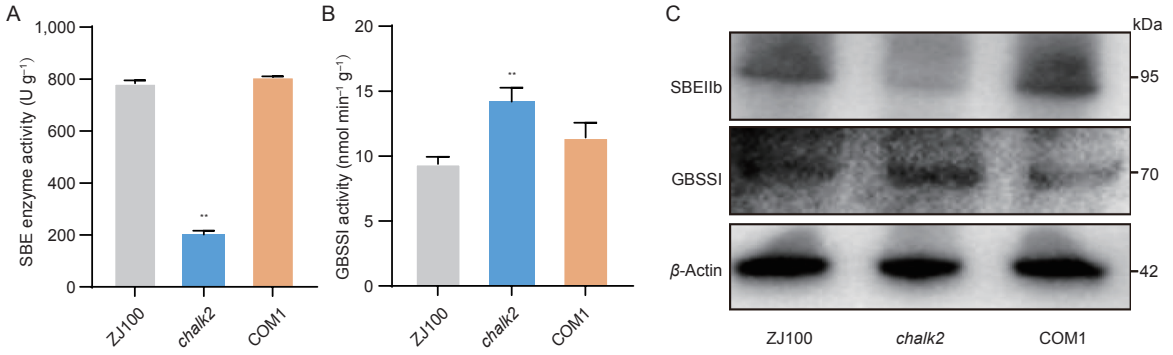


Fig. 5 Analysis of enzymatic activities and Western blot. A, starchbranching enzymes (SBE) activities in Zhongjian 100 (ZJ100), *chalk2* and COM1. B, granule-bound starch synthase I (GBSSI) enzymatic activities in ZJ100, *chalk2* and COM1. Grains of 10 days after fertilization (DAF) were used for enzyme extraction. Bars are SD from at least three replicates. ** indicates significant differences at $P<0.01$ by the two-tailed Student's *t*-test. C, immunoblot analysis of SBE and GBSSI protein abundance in endosperms. *β-Actin* was used as the loading control.

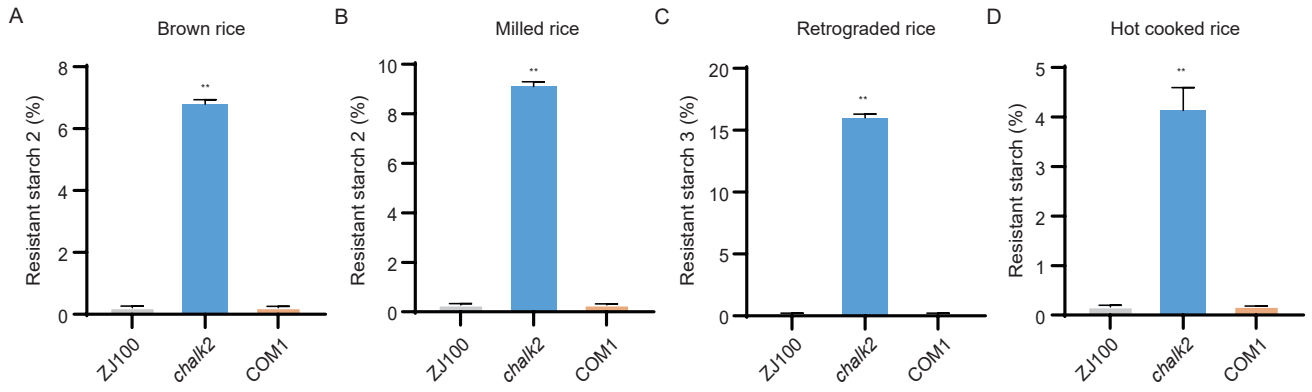


Fig. 6 Content of resistant starch in different types of rice. A and B, content of resistant starch 2 in the brown rice (A) and milled rice (B) of Zhongjian 100 (ZJ100), *chalk2*, and COM1. C, content of resistant starch 3 in the retrograded rice of ZJ100, *chalk2*, and COM1. D, content of resistant starch in the hot-cooked rice of ZJ100, *chalk2*, and COM1. Bars are SD from at least three replicates. ** indicates significant differences at $P<0.01$ by the two-tailed Student's *t*-test.

process of grain filling essentially involves the conversion of carbohydrates into starch, which is then stored in the grain (Nakamura *et al.* 2022). Starch is primarily composed of amylose and amylopectin (Crofts *et al.* 2017). *SBE* is responsible for connecting glucose molecules into linear chains to form branched structures during starch synthesis (Nakamura 2023), and proper branching is essential for effective starch accumulation and granule maturation (Tang and Zhang 2023). The loss of *OsSBEIIb* disrupts the normal branching structure of starch granules, leading to a dramatic increase in amylose content (Butardo *et al.* 2012; Luo *et al.* 2020). In addition to changes in amylose content, the levels of total starch, lipids, and proteins also varied, indicating that *OsSBEIIb* not only affects starch granule structure but also influences the distribution of carbohydrates, causing changes in other nutritional qualities (Wang A *et al.* 2023; Wang A Q *et al.* 2024). In this study, we identified a novel *OsSBEIIb* allele from an EMS-induced *indica* rice mutant library, which has not been previously reported. The serine-to-asparagine substitution observed in this mutant occurs at a highly conserved site (Fig. 4-C; Appendix B), which plays a critical role in starch branching enzyme activity. In the *chalk2* mutant, the total starch and lipid contents were reduced, while the amylose and protein contents increased (Fig. 2-G–J). *OsSBEIIb* also affects the appearance quality, with a noticeable increase in opaque seeds, which is closely linked to the structural changes in starch granules (Nagamatsu *et al.* 2022). Scanning electron microscopy revealed that the starch granules in the mutant were spherical and loosely arranged (Fig. 2-A and B), suggesting that the *OsSBEIIb* mutation leads to reduced branching in starch granules (Nakamura *et al.* 2020), resulting in abnormal granule structure. Furthermore, amylose content typically affects the cooking and eating qualities of rice. Reports have shown that mutations in *OsSBEIIb* lead to a higher gelatinization temperature and changes in rice viscosity (Luo *et al.* 2015; Griebel *et al.* 2019; Ikegaya and Ashida 2021), which are consistent with our findings (Fig. 2-L–N). We hypothesize that these changes are related to the higher amylose content, as amylose molecules are longer and more tightly packed, requiring higher temperatures for dissolution. Taken together, our results suggest that *OsSBEIIb* plays a crucial role in starch synthesis and quality formation in rice, providing new insights for further rice variety improvement.

4.2. Loss of *OsSBEIIb* function increases the resistant starch content in *indica* rice

RS, a beneficial trait for human health, is a form of starch that is resistant to digestion and absorption in the small intestine. It improves gut microbiota and helps control blood sugar levels (DeMartino and Cockburn 2020). However, only a few foods, such as oats, sorghum, barley, legumes, and potatoes, contain substantial amounts of resistant starch (Raigond *et al.* 2015). Therefore, breeding rice varieties with a high resistant starch content is of great importance. Previous studies have reported that starch biosynthesis genes are involved in resistant starch formation. The RS content is reportedly regulated by the *Wx* gene in rice (Bao *et al.* 2017). The *Wxa* allele significantly increases the amylose and resistant starch contents in rice grains (Itoh *et al.* 2003; Zhang *et al.* 2022). Genes from the SS family, particularly *SSSIIIa* and *SSSIIIb*, are associated with the synthesis of resistant starch (Toyosawa *et al.* 2016; Wang A *et al.* 2023). Many studies have demonstrated that a lack of *SBEIIb* activity leads to an increase in resistant starch in the rice endosperm, especially in *japonica* rice (Guo *et al.* 2020; Fujita *et al.* 2022). However, most research on resistant starch has been conducted in *japonica* rice, with limited studies in *indica* rice. This difference is likely due to variations in starch composition and synthesis mechanisms between *indica* and *japonica* rice (Kang *et al.* 2006; Jang *et al.* 2016; Inukai 2017; Deng *et al.* 2024).

In this study, the *chalk2* mutant of *indica* rice showed significantly higher contents of RS2 (resistant starch 2) in brown and milled rice, RS3 (resistant starch 3) in retrograded rice, and resistant starch in hot-cooked rice, compared to the WT ZJ100 (Fig. 6-A–D). Amylopectin, the main component of starch, forms a double helix through its branched structure. During gelatinization, the starch absorbs water and unravels,

making it easier to digest. Upon cooling, the branches reform a double helix structure, producing retrograde starch. Shorter amylopectin branches lead to easier gelatinization and slower retrogradation, making the starch more prone to degradation. In contrast, longer branches make starch harder to gelatinize, accelerate retrogradation, and increase resistance to degradation (Raigond *et al.* 2015; Takahashi and Fujita 2017). Previous studies suggested that *OsSBEIIb* plays a crucial role in controlling the synthesis of shorter amylopectin chains (Nakamura *et al.* 2010). In the current study, when *OsSBEIIb* function was lost, the content of resistant starch increased significantly in the mutant (Fig. 6-C). The altered expression levels of *ISA1* and *ISA2*, the significant downregulation of *SBEI* and *SBEIIa*, the marked upregulation of *SSIIIa* and *SSIIIb*, and the significant increase in *GBSSI* expression (Fig. 7) collectively contributed to starch composition changes in the *chalk2* mutant. These changes led to a reduction in short-chain amylopectin, the formation of long-chain amylopectin (Fig. 2-O), and a higher amylose content (Fig. 2-H). These genes regulate starch composition through distinct mechanisms, ultimately influencing starch granule structure and promoting the formation of RS in *chalk2*. These findings further confirm the critical role of *OsSBEIIb* in regulating *indica* starch branching. Importantly, our findings provide new insights into the role of *OsSBEIIb* in *indica* rice, which highlights the distinct potential of *indica* rice for breeding high resistant starch varieties.

4.3. Germplasm innovation for high resistant starch (RS) varieties

While the contents of resistant starch and amylose increased, other agronomic traits, such as the seed-setting rate and thousand-grain weight (Fig. 1-H and L), were significantly reduced in the *chalk2* mutant compared to ZJ100, resulting in a reduction in individual plant yield (Fig. 1-M). Similar findings have been reported in previous studies, where resistant starch increased but yield decreased (Wang A *et al.* 2023; Wang A Q *et al.* 2024). Interestingly, research has suggested that an RS content of around 10% is a critical threshold, where the yield per plant increases when RS content is below 10%, but plateaus once its content exceeds this value (Wang A Q *et al.* 2024). Yield losses due to high RS content also vary across different rice backgrounds. For instance, in the *ssiiia* and *ssiiib* double mutants, the thousand-grain weight in the *japonica* rice background was lower than that in the *indica* rice background (Huang *et al.* 2024). Therefore, creating high-RS rice varieties with minimal yield loss holds immense value. Previous studies have also shown that hybrids between high-RS mutants and elite rice varieties can maintain yield while improving the resistant starch content (Miura *et al.* 2022). This study created a valuable *indica* rice germplasm with high resistant starch content, which shows potential for use in breeding. The *chalk2* mutant, as a resource with an elevated RS content, represents an important step forward in improving the nutritional quality of rice while minimizing the negative impact on yield. This material can be especially useful for developing high-RS rice varieties in *indica* backgrounds, where resistant starch breeding has been less thoroughly explored compared to *japonica* rice.

5. Conclusion

In this study, a highly chalky mutant, *chalk2*, was identified from the mutant library of the *indica* rice variety ZJ100. The starch composition of the mutant was significantly altered, with marked increases in both the amylose and resistant starch contents. The *chalk2* mutation, caused by disruption of the starch branching enzyme gene *OsSBEIIb*, led to reduced branching of the starch granules, thereby altering the overall starch structure. This novel *indica* rice germplasm with a high resistant starch content has valuable potential for future breeding programs aimed at developing nutritionally improved rice varieties. Furthermore, this research offers new insights for integrating high resistant starch traits into elite varieties, which could be beneficial for populations in need of greater resistant starch intake.

Acknowledgements

This work was supported by grants from the National Natural Science Foundation of China (32372099 and 32188102), the Natural Science Foundation of Zhejiang Province, China (LQ24C130007), and the Innovation Program of Chinese Academy of Agricultural Sciences (CAAS-CSCB-202402).

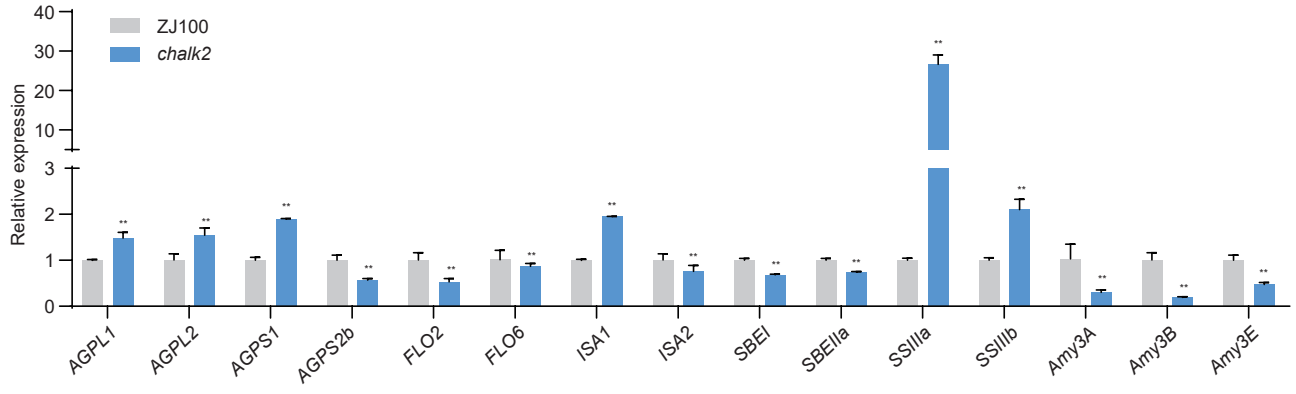


Fig. 7 Expression levels of key starch synthesis genes in Zhongjian 100 (ZJ100) and *chalk2*. Bars are SD from at least three replicates. ** indicates significant differences at $P<0.01$ by the two-tailed Student's *t*-test.

We thank the Public Laboratory of China National Rice Research Institute for their technical support in the subcellular localization studies.

Declaration of competing interest

The authors declare that they have no conflict of interest.

Declaration of generative AI and AI-assisted technologies in the writing process

The authors declare that they did not use AI in the preparation and writing of this manuscript.

Appendices associated with this paper are available at https://doi.org/10.1016/j.jia.2025.04.026

References

Abe A, Kosugi S, Yoshida K, Natsume S, Takagi H, Kanzaki H, Matsumura H, Yoshida K, Mitsuoka C, Tamiru M. 2012. Genome sequencing reveals agronomically important loci in rice using MutMap. *Nature Biotechnology*, **30**, 174–178.

Amagliani L, O'Regan J, Kelly A L, O'Mahony J A. 2016. Chemistry, structure, functionality and applications of rice starch. *Journal of Cereal Science*, **70**, 291–300.

Annison G, Illman R J, Topping D L. 2003. Acetylated, propionylated or butyrylated starches raise large bowel short-chain fatty acids preferentially when fed to rats. *The Journal of Nutrition*, **133**, 3523–3528.

Bao J, Zhou X, Xu F, He Q, Park Y J. 2017. Genome-wide association study of the resistant starch content in rice grains. *Starch-Stärke*, **69**, 1600343.

Bird A R, Flory C, Davies D A, Usher S, Topping D L. 2004. A novel barley cultivar (Himalaya 292) with a specific gene mutation in starch synthase IIa raises large bowel starch and short-chain fatty acids in rats. *The Journal of Nutrition*, **134**, 831–835.

Biswas S, Ibarra O, Shaphek M, Molina-Risco M, Faion-Molina M, Bellinatti-Della Gracia M, Thomson M J, Septiningsih E M. 2023. Increasing the level of resistant starch in 'Presidio' rice through multiplex CRISPR-Cas9 gene editing of starch branching enzyme genes. *Plant Genome*, **16**, e20225.

Deng B W, Zhang Y N, Zhang F, Wang W S, Xu J L, Yu Z, Bao J S. 2024. Genome-wide association study of cooked rice textural attributes and starch physicochemical properties in *indica* rice. *Rice Science*, **31**, 300–316.

Butardo Jr V M, Daygon V D, Colgrave M L, Campbell P M, Resurreccion A, Cuevas R P, Jobling S A, Tetlow I, Rahman S, Morell M, Fitzgerald M. 2012. Biomolecular analyses of starch and starch granule proteins in the high-amylose rice mutant Goami 2. *Journal of Agricultural and Food Chemistry*, **60**, 11576–11585.

Butardo V M, Fitzgerald M A, Bird A R, Gidley M J, Flanagan B M, Larroque O, Resurreccion A P, Laidlaw H K, Jobling S A, Morell M K. 2011. Impact of down-regulation of starch branching enzyme IIb in rice by artificial microRNA-and hairpin RNA-mediated RNA silencing. *Journal of Experimental Botany*, **62**, 4927–4941.

Chisbert M, Castell A L, Vinoy S, Nazare J A. 2024. The impact of slowly digestible and resistant starch on glucose homeostasis and insulin resistance. *Current Opinion in Clinical Nutrition and Metabolic Care*, **27**, 338–343.

Crofts N, Nakamura Y, Fujita N. 2017. Critical and speculative review of the roles of multi-protein complexes in starch biosynthesis in cereals. *Plant Science*, **262**, 1–8.

Cummings J H, Englyst H N. 1991. Measurement of starch fermentation in the human large intestine. *Canadian Journal of Physiology and Pharmacology*, **69**, 121–129.

DeMartino P, Cockburn D W. 2020. Resistant starch: Impact on the gut microbiome and health. *Current Opinion in Biotechnology*, **61**, 66–71.

Fujita N, Miura S, Crofts N. 2022. Effects of various allelic combinations of starch biosynthetic genes on the properties of endosperm starch in rice. *Rice*, **15**, 24.

Griebel S, Westerman R P, Adeyanju A, Addo-Quaye C, Craig B A, Weil C F, Cunningham S M, Patel B, Campanella O H, Tuinstra M R. 2019. Mutations in sorghum *SBEIIb* and *SSIIa* affect alkali spreading value, starch composition, thermal properties and flour viscosity. *Theoretical and Applied Genetics*, **132**, 3357–3374.

Guo D, Ling X, Zhou X, Li X, Wang J, Qiu S, Yang Y, Zhang B. 2020. Evaluation of the quality of a high-resistant starch and low-glutelin rice (*Oryza sativa* L.) generated through CRISPR/Cas9-mediated targeted mutagenesis. *Journal of Agricultural and Food Chemistry*, **68**, 9733–9742.

Huang L, Xiao Y, Zhao W, Rao Y, Shen H, Gu Z, Fan X, Li Q, Zhang C, Liu Q. 2024. Creating high-resistant starch rice by simultaneous editing of *ss3a* and *ss3b*. *Plant Biotechnology Journal*, **22**, 787.

Ikegaya T, Ashida K. 2021. Genetic region responsible for the differences of starch properties in two glutinous rice cultivars in Hokkaido, Japan. *Breeding Science*, **71**, 375–383.

Inukai T. 2017. Differential regulation of starch-synthetic gene expression in endosperm between *indica* and *japonica* rice cultivars. *Rice*, **10**, 1–10.

Itoh K, Ozaki H, Okada K, Hori H, Takeda Y, Mitsui T. 2003. Introduction of *Wx* transgene into rice *wx* mutants leads to both high-and low-amylose rice. *Plant and Cell Physiology*, **44**, 473–480.

Jang E H, Lee S J, Hong J Y, Chung H J, Lee Y T, Kang B S, Lim S T. 2016. Correlation between physicochemical properties of *japonica* and *indica* rice starches. *LWT-Food Science and Technology*, **66**, 530–537.

Kang H G, Park S, Matsuoka M, An G. 2005. White-core endosperm floury *endosperm-4* in rice is generated by knockout mutations in the C_4-type pyruvate orthophosphate dikinase gene (*OsPPDKB*). *The Plant Journal*, **42**, 901–911.

Kang H J, Hwang I K, Kim K S, Choi H C. 2006. Comparison of the physicochemical properties and ultrastructure of *japonica* and *indica* rice grains. *Journal of Agricultural and Food Chemistry*, **54**, 4833–4838.

Kim M K, Park J, Kim D M. 2024. Resistant starch and type 2 diabetes mellitus: Clinical perspective. *Journal of Diabetes Investigation*, **15**, 395–401.

Li J, Jiao G, Sun Y, Chen J, Zhong Y, Yan L, Jiang D, Ma Y, Xia L. 2021. Modification of starch composition, structure and properties through editing of *TaSBEIIa* in both winter and spring wheat varieties by CRISPR/Cas9. *Plant Biotechnol Journal*, **19**, 937–951.

Long X K, Guan C M, Wang L, Jia L T, Fu X J, Lin Q L, Huang Z Y, Liu C. 2023. Rice storage proteins: Focus on composition, distribution, genetic improvement and effects on rice quality. *Rice Science*, **30**, 207–221.

Luo J, Butardo Jr V M, Yang Q, Konik-Rose C, Colgrave M L, Millar A, Jobling S A, Li Z. 2020. The impact of the *indica* rice *SSIIa* allele on the apparent high amylose starch from rice grain with downregulated *japonica SBEIIb*. *Theoretical and Applied Genetics*, **133**, 2961–2974.

Luo J, Jobling S A, Millar A, Morell M K, Li Z. 2015. Allelic effects on starch structure and properties of six starch biosynthetic genes in a rice recombinant inbred line population. *Rice*, **8**, 15.

Miao M, Hamaker B R. 2021. Food matrix effects for modulating starch bioavailability. *Annual Review of Food Science & Technology*, **12**, 169–191.

Miura S, Narita M, Crofts N, Itoh Y, Hosaka Y, Oitome N F, Abe M, Takahashi R, Fujita N. 2022. Improving agricultural traits while maintaining high resistant starch content in rice. *Rice*, **15**, 28.

Nagamatsu S, Wada T, Matsushima R, Fujita N, Miura S, Crofts N, Hosaka Y, Yamaguchi O, Kumamaru T. 2022. Mutation in *BEIIb* mitigates the negative effect of the mutation in *ISA1* on grain filling and amyloplast formation in rice. *Plant Molecular Biology*, **108**, 497–512.

Nakamura Y. 2023. A model for the reproduction of amylopectin cluster by coordinated actions of starch branching enzyme isoforms. *Plant Molecular Biology*, **112**, 199–212.

Nakamura Y, Ono M, Hatta T, Kainuma K, Yashiro K, Matsuba G, Matsubara A, Miyazato A, Mizutani G. 2020. Effects of BEIIb-deficiency on the cluster structure of amylopectin and the internal structure of starch granules in endosperm and culm of *japonica*-type rice. *Frontiers in Plant Science*, **11**, 571346.

Nakamura Y, Steup M, Colleoni C, Iglesias A A, Bao J, Fujita N, Tetlow I. 2022. Molecular regulation of starch metabolism. *Plant Molecular Biology*, **108**, 289–290.

Nakamura Y, Utsumi Y, Sawada T, Aihara S, Utsumi C, Yoshida M, Kitamura S. 2010. Characterization of the reactions of starch branching enzymes from rice endosperm. *Plant and Cell Physiology*, **51**, 776–794.

Nishi A, Nakamura Y, Tanaka N, Satoh H. 2001. Biochemical and genetic analysis of the effects of amylose-extender mutation in rice endosperm. *Plant Physiology*, **127**, 459–472.

Ohdan T, Francisco Jr P B, Sawada T, Hirose T, Terao T, Satoh H, Nakamura Y. 2005. Expression profiling of genes involved in starch synthesis in sink and source organs of rice. *Journal of Experimental Botany*, **56**, 3229–3244.

Pugh J E, Cai M, Altieri N, Frost G. 2023. A comparison of the effects of resistant starch types on glycemic response in individuals with type 2 diabetes or prediabetes: A systematic review and meta-analysis. *Frontiers in Nutrition*, **10**, 1118229.

Raigond P, Ezekiel R, Raigond B. 2015. Resistant starch in food: A review. *Journal of the Science of Food and Agriculture*, **95**, 1968–1978.

Sajilata M G, Singhal R S, Kulkarni P R. 2006. Resistant starch — A review. *Comprehensive Reviews in Food Science and Food Safety*, **5**, 1–17.

Sawada T, Itoh M, Nakamura Y. 2018. Contributions of three starch branching enzyme isozymes to the fine structure of amylopectin in rice endosperm. *Frontiers in Plant Science*, **9**, 1536.

Sun Y, Jiao G, Liu Z, Zhang X, Li J, Guo X, Du W, Du J, Francis F, Zhao Y. 2017. Generation of high-amylose rice through CRISPR/Cas9-mediated targeted mutagenesis of starch branching enzymes. *Frontiers in Plant Science*, **8**, 298.

Takahashi T, Fujita N. 2017. Thermal and rheological characteristics of mutant rice starches with widespread variation of amylose content and amylopectin structure. *Food Hydrocolloids*, **62**, 83–93.

Tang Z, Zhang D. 2023. Research progress on the molecular mechanism of starch accumulation in rice endosperm. *Chinese Bulletin of Botany*, **58**, 612–621.

Tappiban P, Hu Y, Deng J, Zhao J, Ying Y, Zhang Z, Xu F, Bao J. 2022. Relative importance of branching enzyme isoforms in determining starch fine structure and physicochemical properties of *indica* rice. *Plant Molecular Biology*, **108**, 399–412.

Toyosawa Y, Kawagoe Y, Matsushima R, Crofts N, Ogawa M, Fukuda M, Kumamaru T, Okazaki Y, Kusano M, Saito K. 2016. Deficiency of starch synthase IIIa and IVb alters starch granule morphology from polyhedral to spherical in rice endosperm. *Plant Physiology*, **170**, 1255–1270.

Turker B, Savlak N Y. 2015. Resistant starch: Types, sources, beneficial physiological effects and functional properties. *Akademik Gida*, **13**, 354–359.

Utsumi Y, Utsumi C, Tanaka M, Takahashi S, Okamoto Y, Ono M, Nakamura Y, Seki M. 2022. Suppressed expression of starch branching enzyme 1 and 2 increases resistant starch and amylose content and modifies amylopectin structure in cassava. *Plant Molecular Biology*, **108**, 413–427.

Wada T, Yamaguchi O, Miyazaki M, Miyahara K, Ishibashi M, Aihara T, Shibuta T, Inoue T, Tsubone M, Toyosawa Y. 2018. Development and characterization of a new rice cultivar,'Chikushi-kona 85', derived from a starch-branching enzyme IIb-deficient mutant line. *Breeding Science*, **68**, 278–283.

Wang A, Jing Y, Cheng Q, Zhou H, Wang L, Gong W, Kou L, Liu G, Meng X, Chen M, Ma H, Shu X, Yu H, Wu D, Li J. 2023. Loss of function of SSIIIa and SSIIIb coordinately confers high RS content in cooked rice. *Proceedings of the National Academy of Sciences of the United States of America*, **120**, e2220622120.

Wang B, Liu J, Chen X L, Xu Q, Zhang Y Z, Dong H X, Tang H P, Qi P F, Deng M, Ma J, Wang J R, Chen G Y, Wei Y M, Zheng Y L, Jiang Q T. 2025. A barley *SS2a* single base mutation at the splicing site leads to obvious changes in starch. *Journal of Integrative Agriculture*, **24**, 1359–1371.

Wang A Q, Cheng Q, Li W J, Kan M X, Zhang Y X, Meng X B, Guo H Y, Jing Y H, Chen M J, Liu G F, Wu D X, Li J Y, Yu H. 2024. Creation of high-resistant starch rice through systematic editing of amylopectin biosynthetic genes in *rs4*. *Plant Biotechnology Journal*, **23**, 480–488.

Wang F X, Mo J H, Hu X Z, Ma Z. 2024. The degradation mechanism of resistant starch by human gut microflora. *Journal of Chinese Institute of Food Science and Technology*, **24**, 364–378.

Wang L, Liu L L, Zhao J L, Li C L, Wu H L, Zhao H X, Wu Q. 2023. Granule-bound starch synthase in plants: Towards an understanding of their evolution, regulatory mechanisms, applications, and perspectives. *Plant Science*, **336**, 111843.

Wei X, Jiao G, Lin H, Sheng Z, Shao G, Xie L, Tang S, Xu Q, Hu P. 2017. *GRAIN INCOMPLETE FILLING 2* regulates grain filling and starch synthesis during rice caryopsis development. *Journal of Integrative Plant Biology*, **59**, 134–153.

Wen J J, Li M Z, Nie S P. 2023. Dietary supplementation with resistant starch contributes to intestinal health. *Current Opinion in Clinical Nutrition and Metabolic Care*, **26**, 334–340.

Yamanouchi H, Nakamura Y. 1992. Organ specificity of isoforms of starch branching enzyme (Q-enzyme) in rice. *Plant and Cell Physiology*, **33**, 985–991.

Zhang Q. 2024. Research progress on the regulatory effect of resistant starch on type 2 diabetes mellitus and its mechanism. *Journal of Food Safety and Quality*, **15**, 250–259.

Zhang Z, Hu Y, Zhao J, Zhang Y, Ying Y, Xu F, Bao J. 2022. The role of different *Wx* and *BEIIb* allele combinations on fine structures and functional properties of *indica* rice starches. *Carbohydrate Polymers*, **278**, 118972.

Executive Editor-in-Chief Xueyong Zhang
Managing Editor Ning Wang